

This is a repository copy of *Rods to discs in the study of mesomorphism in discotic liquid crystals*.

White Rose Research Online URL for this paper:

<https://eprints.whiterose.ac.uk/137931/>

Version: Published Version

Article:

Zhong, Tingjun, Mandle, Richard orcid.org/0000-0001-9816-9661, Saez, Isabel orcid.org/0000-0002-2252-6228 et al. (2 more authors) (2018) Rods to discs in the study of mesomorphism in discotic liquid crystals. LIQUID CRYSTALS. pp. 2274-2293. ISSN 1366-5855

<https://doi.org/10.1080/02678292.2018.1515371>

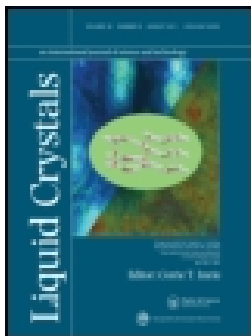
Reuse

This article is distributed under the terms of the Creative Commons Attribution (CC BY) licence. This licence allows you to distribute, remix, tweak, and build upon the work, even commercially, as long as you credit the authors for the original work. More information and the full terms of the licence here:

<https://creativecommons.org/licenses/>

Takedown

If you consider content in White Rose Research Online to be in breach of UK law, please notify us by emailing eprints@whiterose.ac.uk including the URL of the record and the reason for the withdrawal request.



Rods to discs in the study of mesomorphism in discotic liquid crystals

Tingjun Zhong, Richard Mandle, Isabel Saez, Stephen Cowling & John Goodby

To cite this article: Tingjun Zhong, Richard Mandle, Isabel Saez, Stephen Cowling & John Goodby (2018): Rods to discs in the study of mesomorphism in discotic liquid crystals, *Liquid Crystals*, DOI: [10.1080/02678292.2018.1515371](https://doi.org/10.1080/02678292.2018.1515371)

To link to this article: <https://doi.org/10.1080/02678292.2018.1515371>



© 2018 The Author(s). Published by Informa UK Limited, trading as Taylor & Francis Group.



Published online: 18 Sep 2018.



Submit your article to this journal [↗](#)





Article views: 170



View Crossmark data [↗](#)

Rods to discs in the study of mesomorphism in discotic liquid crystals

Tingjun Zhong, Richard Mandle , Isabel Saez, Stephen Cowling  and John Goodby

Department of Chemistry, The University of York, York, UK

ABSTRACT

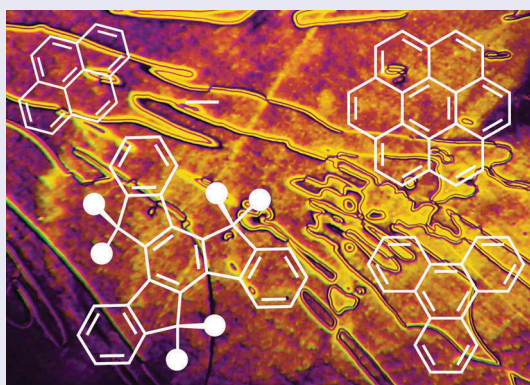
The rational design of calamitic liquid crystals is an area of research that has been intensively explored due to their extensive applications in various devices. The successful methods for design have been, to some extent, mapped on discotic systems such that certain features of the structures of calamitic phases have been superimposed upon those of nematic discotic and columnar phases. In this article, we explore the correlation between nematogenic behaviour of hard rod-like particles and that of hard disc-like systems. We show that for calamitics, nematic behaviour is observed, whereas for discotics this is not the case. Furthermore, we show that nematic discotic materials are miscible, whereas unlike smectics, columnar phases are less likely to be miscible. Indeed, it appears that columnar discotic phases are greater similarities with soft-solids than true liquid crystals.

ARTICLE HISTORY

Received 15 June 2018

KEYWORDS

Discotics; amphiphiles;
phase diagrams; eutectics



Introduction

Theoretical modelling of liquid crystals usually starts with assuming that the molecules are effectively particles with anisotropic shapes, with rod-like topologies being the most preferred. This assumption has been very successful in classifying calamitic liquid crystals by the extent and arrangement of positional ordering of the molecules. The extent of the ordering can be short-range, long-range, or with geometric decay as described by Leadbetter [1]. Hierarchical structuring can be additionally superimposed via the nature of layering (sinusoidal) and orientational arrangements of the molecules (orthogonal or tilted). This almost-complete picture of the possibilities for the arrangements of rod-like molecules in soft-matter phases is depicted in Figure 1 [2,3]. The understanding of the structures and properties of some of the phases have led to a wide variety of applications of liquid crystals,

from displays, light modulators and imaging devices to high-yield strength materials, attenuators and artificial muscle.

The success of the theoretical models [4–10] and subsequent simulations coupled with experiment and analysis has resulted in a tendency to transfer theoretical concepts and models to other aspects of liquid crystals. One set of examples is that of mesophases composed of disc-like entities [11–13]. With the discovery of discotic phases, there came with them a view that there must be analogies with mesophases of rod-like systems. Figure 2, although incomplete and possibly subject to error, shows a depiction for the phases of disc-like molecules in comparison with those of calamitic systems. Without fully understanding the structures of the mesophases formed by disc-like entities, they have nevertheless found uses in a number of applications, such as optical compensation films [14],

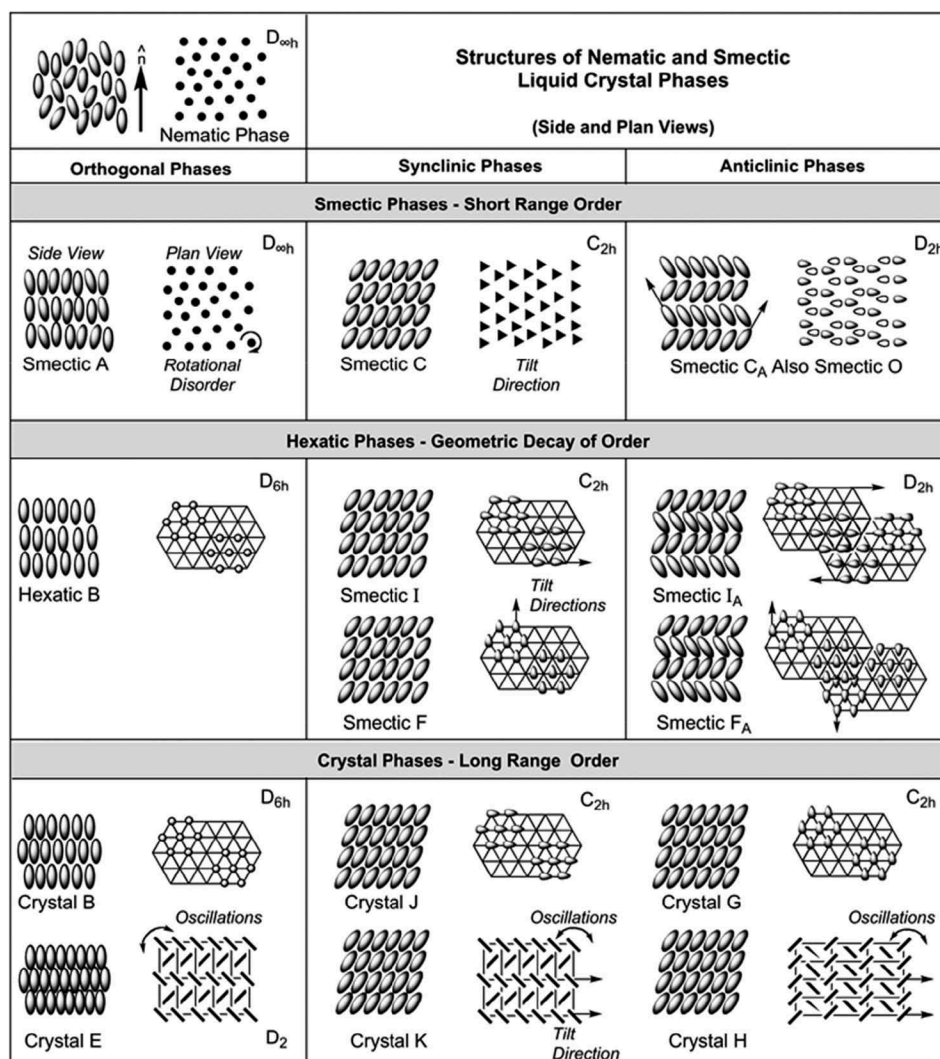


Figure 1. Schematic depiction of the organisation of the rod-like molecules in the formation of calamitic mesophases [3].

high-performance lubricants [15], semi-conductors [16] and non-linear optical (NLO) materials [17].

One of the earliest investigations of the mesophases formed by disc-like molecules was made in the petrochemical industries where nematic liquid crystals were found to be formed by the heavy ends of oils. These mesophases were later called Carbonaceous Mesophases.

In the 1960s, White et al. demonstrated mesophase transformation occurring in graphitisable organic materials during pyrolysis at temperatures of around 450°C [18]. They postulated that the mesophase was a two-phase, liquid-state and the structural transition involved sheet-like molecules being aligned in a parallel array to form a liquid crystal. Polarised optical microscopy (POM) gave an image of a *schlieren* texture of the nematic phase with two-brush and four-brush disclinations, as shown in Figure 3. Similarly, several other groups have also reported on the mesophase transformation taking

place during carbonisation between temperatures of 350°C and 500°C [19–22].

It was also thought that graphitisation occurred via solidification from the liquid phase mediated by a mesophase having properties similar to those of liquid crystals, whereby during thermal cracking process aromatic polymerisation and carbonisation produced graphitic organic materials [23].

One of the earliest theoretical models used to describe liquid crystal phases was Onsager's [7], which described lyotropic liquid crystals [24] via a hard-rod model where the volume excluded from the centre-of-mass of one idealised cylinder was considered as it approached another. Thus, the parallel arrangement of anisotropic objects led to a decrease in orientational entropy, but conversely there was an increase in positional entropy. If we now consider Onsager's model and draw a direct comparison between calamitic

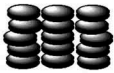
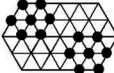

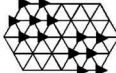

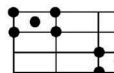



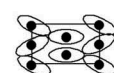

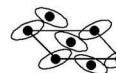

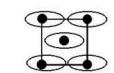

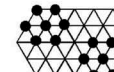

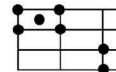
| Orthogonal Phases | | Tilted Phases | | | |
|--|---|---|---|--|--|
| Side View | Plan View | Hexagonal Columnar Phases - Short Range Order along columns | | | |
|  Hexagonal Columnar Disordered |  Col _{hd} D _{6h} |  Hexagonal Tilted Columnar Disordered |  Col _t C _{2h} | | |
| Upright Columnar - Rectangular | | 2D - Tilted Columnar - Rectangular Disordered Mesophases | | | |
|  Rectangular Columnar Disordered |  Col _{rd} D _{2h} |  Rectangular |  Col _{rd} P _{21/a} |  Rectangular |  Col _{rd} P _{2a} |
| | |  Oblique |  Col _{rd} P ₁ |  Rectangular Face centred tilted |  Col _{rd} C _{2/m} |
| Crystal Phases | | Crystal Phases | | | |
|  Hexagonal Columnar Ordered |  Col _{ho} D _{6h} |  Rectangular Columnar Disordered |  Col _{rd} D _{2h} | | |

Figure 2. Schematic depiction of the organisation of the disc-like molecules in the formation of discotic liquid crystals.

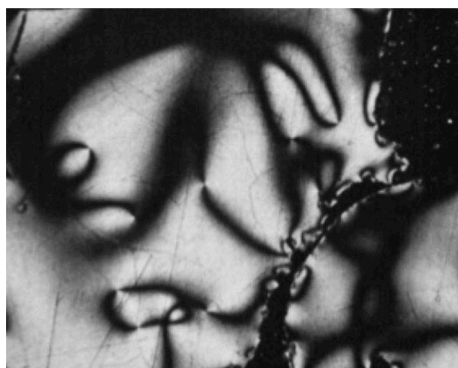


Figure 3. Polarised light micrograph (crossed polarizers) (150 \times) of extracted pitch carbonised to 450 $^{\circ}$ C at approximately 0.4 $^{\circ}$ C/min [18]. Reprinted from Carbon, 5, J.L. White, G. L. Guthrie and J. O. Gardner, "Mesophase microstructures in carbonised coal-tar pitch517-518., 1967, with permission from Elsevier.

and discotic systems, we find that for calamitics the aspect ratio for the rod-like bodies is important in the formation of nematic phases [25]. A simple demonstration of the effects of aspect ratio on nematic phase formation can be gauged from the comparison of the clearing points of some unsubstituted, rigid-rod, oligo-*p*-phenylenes. For example, biphenyl, *p*-terphenyl and *p*-quaterphenyl are not mesogenic because their relative aspect ratios are too small, whereas *p*-quinquephenyl and *p*-sexiphenyl are nematic at high temperatures; see Figure 4 (left-hand column). The higher homologues tend to decompose near to their transitions to the liquid state, although there have been some reports that septiphenyl exhibits liquid crystallinity. However, for the higher polyphenyls, mesomorphic behaviour apparently is not observed. Through the introduction

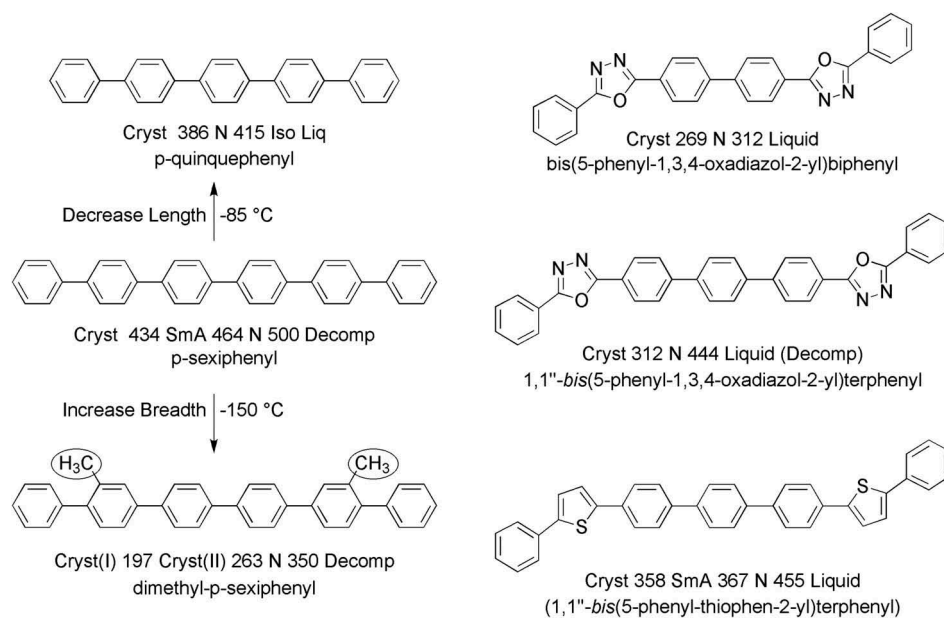


Figure 4. The transition temperatures and melting points (°C) for *p*-quinquephenyl, *p*-sexiphenyl and 2',3'''-dimethyl-*p*-sexiphenyl (left column), and 4,4'-bis(5-phenyl-1,3,4-oxadiazol-2-yl)biphenyl, 1,1''-bis(5-phenyl-1,3,4-oxadiazol-2-yl)terphenyl and 1,1''-bis(5-phenyl-thiophen-2-yl)terphenyl (right column).

of lateral groups to sexiphenyl, we can effectively reduce the aspect ratio simply by increasing the molecular breadth. Consider compound 2',3'''-dimethylsexiphenyl, which also has a rigid structure because it has two methyl groups directly attached to the polyphenyl unit. In a conformational structure, with both methyl groups positioned on the same side of the polyphenyl unit, the aspect ratio will be reduced because the breadth of the molecule is larger and the length is the same. Consequently, the clearing point is lowered relative to *p*-sexiphenyl by 150°C.

The aspect ratio for unsubstituted hard rods can also be decreased via the incorporation of five membered rings, as shown for the structurally related compounds: 4,4'-bis(5-phenyl-1,3,4-oxadiazol-2-yl)biphenyl, 1,1''-bis(5-phenyl-1,3,4-oxadiazol-2-yl)terphenyl and 1,1''-bis(5-phenyl-thiophen-2-yl)terphenyl, as shown in Figure 4 (right-hand column) [26]. These materials have slightly bent structures, which increase the breadth relative to the length, thereby lowering the relative aspect ratio and the relative clearing point with respect to *p*-sexiphenyl [26]. The clearing point for the oxadiazole analogue is 188°C lower than for *p*-sexiphenyl, whereas for the seven-ring oxadiazole (the analogue of septiphenyl), the clearing point of 444°C is similar to that of *p*-sexiphenyl. Similarly, for the analogous seven-ring material, 1,1''-bis(5-phenyl-thiophen-2-yl)terphenyl, the clearing point of 455°C is similar. Thus, the bent shaped seven-ring oxadiazole and thiophene have similar clearing points to the six-ring sexiphenyl indicating that the increase in molecular breadth is effectively equivalent to shortening by

one ring. Moreover, the similarity in the clearing points relative to absolute zero means that molecular shape is potentially more important than electrostatic interactions [25]. In the following, we now consider similar effects for hard and amphiphilic discs.

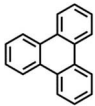
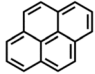
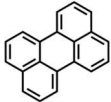
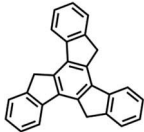
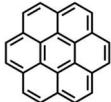
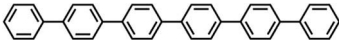
Experimental studies and results

Mesomorphism for hard disc systems

Bearing Onsager theory in mind, if we now turn to disc-like systems and consider the mesomorphic properties of hard discs, we find there are few studies on the behaviours of materials such as triphenylene, truxene, coronene, etc., where the numbers of aromatic rings are similar to those of the mesogenic polyols described above. The structures investigated in this study are given in Table 1, and the minimised geometries optimised at the B3LYP/6-31G(d) level of DFT and Chem Draw for three of the materials are shown in Figure 5. Additionally, the predicted local staggered stacking arrangements of columnar units that could possibly form in condensed phases are also given.

The materials in Table 1 were initially investigated by differential scanning calorimetry (DSC). The results for rod-like *p*-sexiphenyl show two crystal forms on heating, followed by a smectic A to nematic phase transition at approximately 472°C, decomposition then occurs at temperatures above 500°C. The DSC thermograms for the disc-like systems of triphenylene, pyrene, perylene, truxene and coronene are shown

Table 1. The chemical structures, melting points (°C) and associated enthalpies of transition (kJ mol^{-1}) determined for the variety of cyclic and linear polyaromatics under investigation [27–32].

| Compound | Chemical structure | Melting point/ °C |
|----------------------|---|---|
| Triphenylene |  | 197.3 ($\Delta H = 20.6 \text{ kJ mol}^{-1}$) |
| Pyrene |  | 150.2 ($\Delta H = 12.5 \text{ kJ mol}^{-1}$) |
| Perylene |  | 274.9 ($\Delta H = 31.8 \text{ kJ mol}^{-1}$) |
| Truxene |  | 384.7 ($\Delta H = 36.6 \text{ kJ mol}^{-1}$) |
| Coronene |  | 432.9 ($\Delta H = 21.9 \text{ kJ mol}^{-1}$) |
| <i>p</i> -sexiphenyl |  | 439.9 ($\Delta H = 27.8 \text{ kJ mol}^{-1}$) |

together in Figure 6. Each material was also not heated above 490°C because of the potential for decomposition. The first point to note from the data is that triphenylene (3-rings) and pyrene (4-rings) exhibit one crystal phase on heating but two on cooling, and that there was substantial supercooling of the recrystallisation temperature. No mesophases were formed for these first three homologues, which is similar to the behaviour of rod-like systems, for which the melting points and relative enthalpies are similar. Perylene (5-rings), unlike *p*-quinquephenyl was found to be non-mesogenic. The higher homologues, truxene and coronene, exhibited higher melting points (384°C and 433°C respectively), and upon melting, the DSC thermograms show some decomposition, thus on cooling, an enthalpy for solidification was not observed in either of the thermograms. However, their melting temperatures and associated enthalpies are not so dissimilar to those of *p*-sexiphenyl, but in contrast no mesophases were observed for either. Thus, the compounds with disc-like architectures do not appear to exhibit liquid crystal phases. This may be an indicator

that the π face-to-face, interactions may be too strong, even at high temperatures, to allow the molecular discs to diffuse past one another in a nematic phase. This suggests that hard discs may be less likely to form mesophases, and that the intermolecular interactions are more important than for rod-like systems. This may be related to the fact that intermolecular twisting of adjacent phenyl rings in materials such as *p*-sexiphenyl in rod-like systems weakens to some degree the π - π interactions, thereby favouring mesophase formation. The one case where steric interference could occur for the disc-like materials is for truxene, and although the compound appears to be non-mesogenic, it still has interesting properties to which we will return later.

Extrapolation of the values for the virtual clearing points for selected polyaromatics

In 1979, Béguin et al. attempted to investigate discotic mesophase potentiality [34]. They did this by creating two binary phase diagrams in order to determine the virtual discotic liquid crystal to liquid transition for a

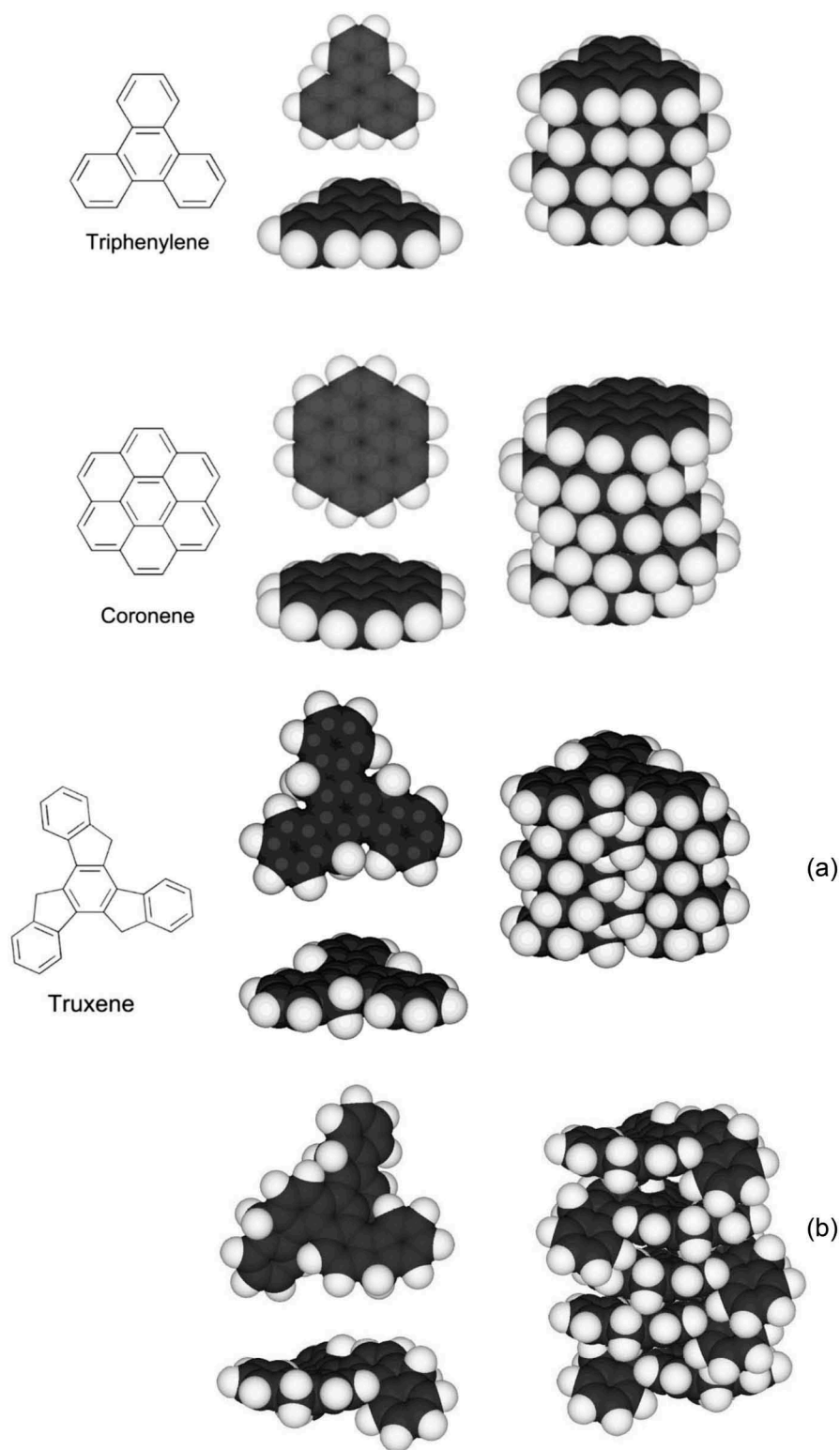


Figure 5. The space-filling structures and face-to-face interactions of triphenylene, coronene and truxene [33]. Truxene has a relatively flat disc-like shape as determined by simulations and crystal structure X-ray determination (a), but at high temperatures, it has the possibility of being slightly twisted out of shape as shown in (b).

compound exhibiting no discotic phases (stable or monotropic). In these studies, they mixed amphiphilic discotic liquid crystal materials with triphenylene and pyrene to determine the virtual phase transition temperatures. They

found that the discotic phase transition for triphenylene was approximately 55°C and for pyrene 80°C. In these studies, they used the penta- and hepta-substituted hexaalkoxytriphenylenes (HATs) in the mixtures [35,36]. The

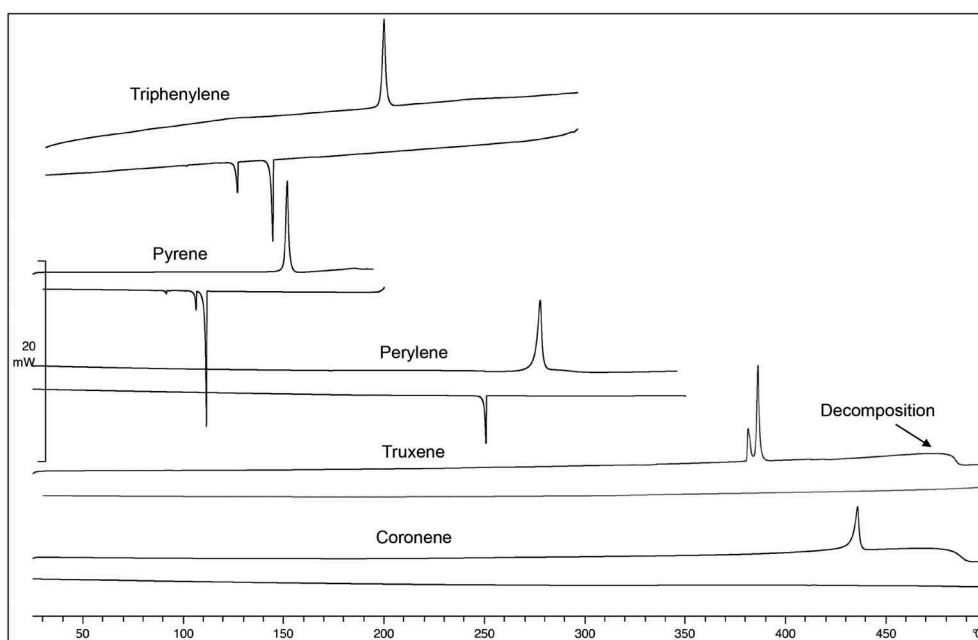


Figure 6. The DSC thermograms as a function of temperature (°C) for triphenylene, pyrene, perylene, truxene and coronene.

HAT materials, however, are known to exhibit columnar phases and not nematic phases, and therefore the results they obtained may reflect a transition to a columnar phase as opposed to a nematic phase – results that may be important in the later discussions.

Thus, two *bonafide* discotic nematogens (one with an additional columnar phase) were used in this present

study as the standard materials in the determination of extrapolated N-I values via the use of Gibbs phase diagrams [36]. In the first instance, triphenylene was used as the target hard disc material for study with compounds **1** and **2** (Figure 7) in binary mixtures.

For the mixtures of triphenylene and compound **1**, their phase behaviours were examined using POM and

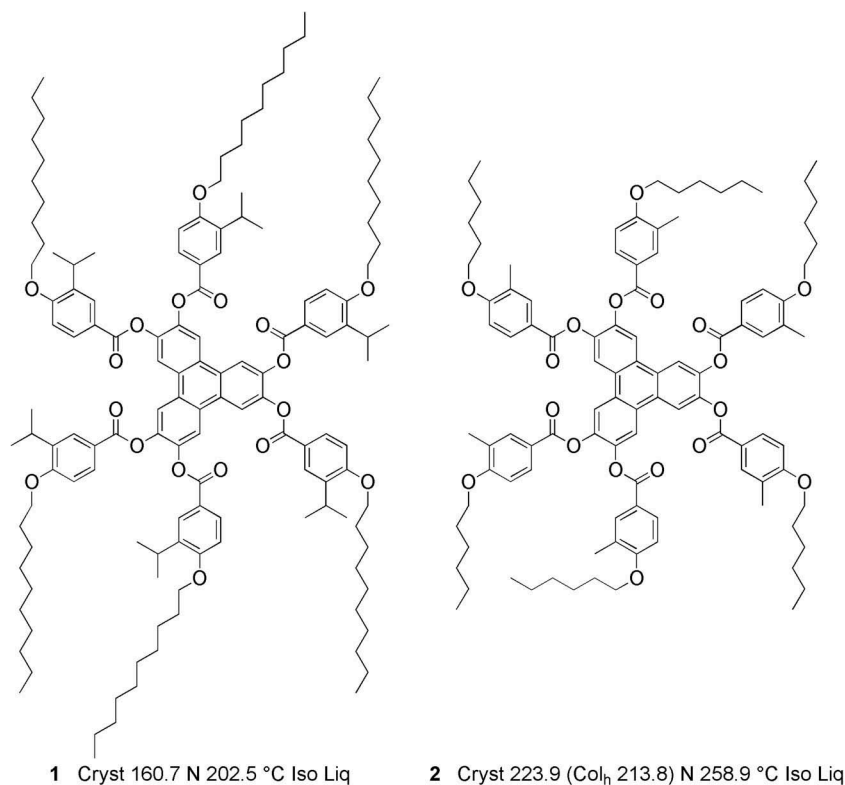


Figure 7. Structures of standard discotic nematic materials **1** and **2** [38–40].

DSC. The transition temperatures for the mixtures are shown in Table 2, and the binary phase diagram for the results is given in Figure 8. In addition, photomicrographs of the defect textures at various concentrations are incorporated into the phase diagram.

In the phase diagram, the melting point curve did not have an obvious eutectic point. Instead, for the concentration range between 50 and 80 mol% of triphenylene, the melting temperatures were similar and the curve bottomed-out indicating that a eutectic point may occur in this region. Conversely, for the nematic to isotropic liquid transition temperature curve, as the concentration of triphenylene was increased, the lower the N-I phase transition became. In addition, at concentrations of 90 mol% or more of triphenylene in the mixtures, no mesophases were observed. However, extrapolation of the N-I curve to 100 mol% of triphenylene showed that triphenylene possesses a virtual N-I point at approximately $135 \pm 10^\circ\text{C}$.

Table 2. Mixture compositions (mol %) and transition temperatures ($^\circ\text{C}$) for binary mixtures of triphenylene and compound 1.

| Compd/Mixture | Triph (mol %) | Cryst | <i>N</i> | Iso Liq |
|---------------|---------------|-------|----------|---------|
| Compd 1 | 0 | . | 160.7 | 202.5 |
| Mix-1 | 10 | . | 156.6 | 199.8 |
| Mix-2 | 30 | . | 139.5 | 189.0 |
| Mix-3 | 50 | . | 123.3 | 176.8 |
| Mix-4 | 70 | . | 123.2 | 156.9 |
| Mix-5 | 80 | . | 127.4 | 152.2 |
| Mix-5 | 90 | . | 158.7 | - |
| Triphenylene | 100 | . | 197.4 | - |

This is reasonable evidence that non-amphiphilic hard-disc molecular systems can potentially exhibit thermotropic mesophases. Conversely, for rod-like systems, this occurs enantiotropically for quinquephenyl between 386°C and 415°C . Nevertheless, the result infers that Onsager theory for hard particles could be applied to particles with disc-like topologies as well as to those that are rod shaped.

Compound 2 was selected to investigate the relationship between nematic and columnar properties of triphenylene because it exhibits a hexagonal columnar phase as well as a nematic phase. The transition temperatures for the various mixtures prepared between triphenylene and compound 2 are given in Table 3, and the phase diagram for mixtures between the two materials, along with photomicrographs, is shown in Figure 9.

The phase diagram for triphenylene and compound 2 shows that the nematic and hexagonal columnar phases were exhibited by mixtures that contained less than 70 mol% of triphenylene. Additionally, the N-I and the N-Col_h phase transition curves showed a fall in value as the concentration of triphenylene was increased. Moreover, no mesophases were observed by mixtures containing above 70 mol% of triphenylene. The phase diagram also shows a potential eutectic point occurring between 70 and 80 mol% of triphenylene. The linear extrapolated N-I phase transition curve

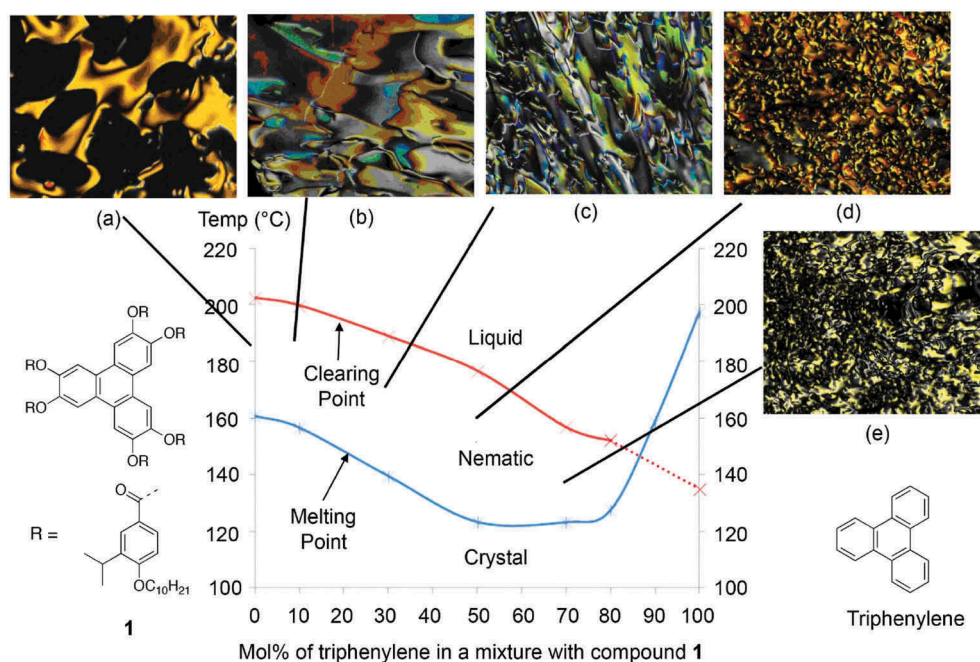


Figure 8. (Colour online) The phase diagram for the binary mixtures of triphenylene and compound 1. Photomicrographs ($\times 100$) Showing optical textures for: (a) Compound 1 cooling, 183.5°C – nematic; (b) 10.0 mol% triphenylene on heating, 178.8°C – nematic; (c) 30.0 mol% triphenylene on cooling, 175.5°C – nematic; (d) 50.0 mol% triphenylene on cooling, 171.0°C – nematic; (e) 70 mol% triphenylene on cooling, 158.0°C – nematic.

Table 3. Mixture compositions (mol %) and transition temperatures (°C) for binary mixtures of triphenylene and compound **2**.

| Compd/Mixture | Triph (mol %) | Cryst 1 | Cryst 2 | Col _h | N | Iso Liq |
|----------------|---------------|---------|---------|------------------|---|---------|
| Compd 2 | 0 | . | 214.1 | - | - | 224.4 |
| Mix- 7 | 10 | . | 210.4 | - | . | 249.4 |
| Mix- 7 | 30 | . | 197.4 | - | . | 238.7 |
| Mix- 9 | 50 | . | 162.0 | - | . | 221.8 |
| Mix- 10 | 70 | . | 130.0 | - | . | 173.9 |
| Mix- 11 | 90 | . | 134.4 | 172.9 | - | - |
| Triphenylene | 100 | . | 197.4 | - | - | - |

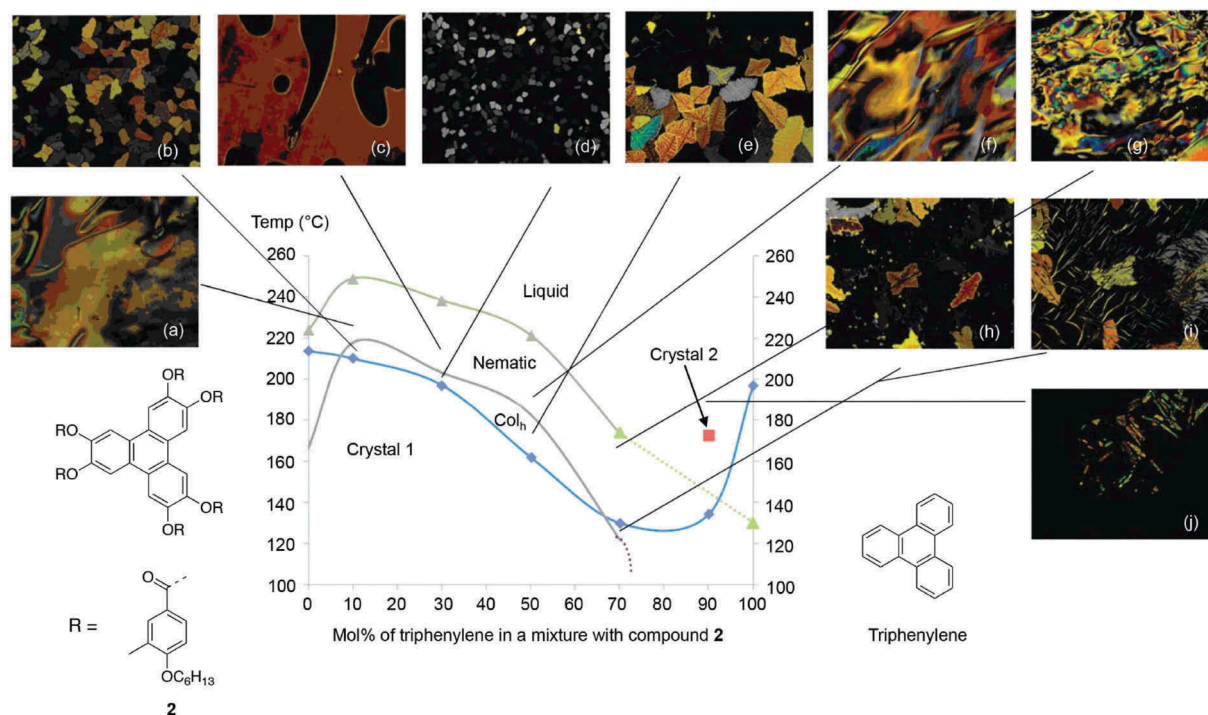


Figure 9. (Colour online) The phase diagram for the binary mixtures of triphenylene and compound **2**. Photomicrographs ($\times 100$) showing optical textures for mixture of compound **2** with: (a) 10 mol% triphenylene on heating, 220°C – nematic; (b) 10 mol% triphenylene on cooling, 215.0°C – Col_h; (c) 30.0 mol% triphenylene on heating, 224.0°C – nematic; (d) 30 mol% triphenylene on cooling, 210.0°C – nematic; (e) 50 mol% triphenylene on cooling, 187.1°C – Col_h; (f) 50 mol% triphenylene on heating, 187.1°C – Col_h; (g) 50.0 mol% triphenylene on heating, 216.3°C – nematic; (h) 70 mol% triphenylene on cooling, 120.0°C – Col_h; (i) 70.0 mol% triphenylene on cooling, 120.0°C – Col_h; (j) 90 mol% triphenylene on heating, 190.0°C.

to 100 mol% of triphenylene gives a virtual N-I phase transition of approximately 135°C, but this value could be much lower if the direction of the transition curve is followed. Conversely, the N-Col_h curve could not be extrapolated to 100 mol% of triphenylene, indicating contrary to Béguin et al [34] that triphenylene does not have any latent columnar phase properties.

These results are similar to those of rod-like systems where only nematic phases are observed for the smaller aromatic systems. However, as the aspect ratios for the rod-like molecules are increased by increasing the number of phenyl units, the introduction of smectic phases results. Thus, it might be expected that as the diameters of the disc-like materials are increased, columnar phases may result.

For binary mixtures of other hard-disc materials with substituted triphenylene derivatives, e.g., compounds **1**

and **2** etc., only substantial mixing was found for triphenylene. For the other polyaromatics, such as pyrene and perylene, mixing was found not to occur with triphenylene derivatives **1** and **2**. Separation was observed by optical microscopy in melting cycles and uncharacteristic DSC thermograms were obtained.

Mixture studies of different hard discs and hard rods

As the evidence for liquid-crystalline behaviour for hard-disc systems was found to be weak, depression of the melting point was sought via the study of eutectic mixtures composed of compounds with preferred structural architectures. A related Schröder-van Laar equation was used to simulate eutectics from the DSC data of the selected compounds, thereby allowing for the preparation of eutectic

mixtures. The results for eutectic mixtures from simulations for three-component, **Mix-12** (all flat disc components), four-component, **Mix-13** (3-flat discs components plus one twisted-disc component) and five-component, **Mix-14** (3 flat and 1-twisted disc components, plus 1-rod-like component) systems are shown in Table 4, as well as the melting points are determined by POM experiments. The results from the DSC experiments are given in Figure 10. All three mixtures melted from the solid to the liquid state with rather large enthalpies of transition ($\Delta H = 110.20, 32.37, 65.46 \text{ Jg}^{-1}$ respectively), and recrystallisations in the cooling cycle were accompanied by substantial supercooling. For **Mix-12** and **Mix-14**, no mesomorphic behaviour was observed; however for **Mix-13**, POM and DSC showed that a possible phase was present between 206°C and 212°C.

For **Mix-13**, a dark texture was observed by POM at approximately 200°C between the solid and liquid states, as shown in Figure 11. It's almost extinct texture (Figure 11(a)) indicates that it is close to being optically isotropic and is probably amorphous in nature. Increasing the power of the light source shows that there is a very faint defect texture (Figure 11(b)), which becomes clearer when the colour of the photograph is inverted (Figure 11(c)). The DSC thermal cycling for **Mix-13** shows that there is a very small enthalpy in the temperature region in which the mesophase was detected by POM. The enthalpy is weak and broad, but nevertheless detectable (shown in Figure 12). This is the first indication that materials with hard-disc chemical structures may be capable of being mesomorphic. Why this might occur upon the addition of truxene to a flat disc-

Table 4. Mixture compositions (mol %), and predicted eutectic point with experimental melting point (°C) for three different mixtures made up of 3, 4 and 5 components.

| Compound in Mixture (mol %) | Mix-12 (3 component) | Mix-13 (4 component) | Mix-14 (5 component) |
|---------------------------------|----------------------|----------------------|----------------------|
| Triphenylene | 70.0 | 67.4 | 64.1 |
| Perylene | 19.3 | 18.4 | 17.2 |
| Coronene | 10.7 | 10.3 | 10.1 |
| Truxene | - | 3.7 | 3.4 |
| <i>p</i> -sexiphenyl | - | - | 5.2 |
| Calculated eutectic point (°C) | 170.0 | 167.5 | 164.1 |
| Actual melting point (°C) (max) | 172.7 | 175.9 | 173.7 |
| $\Delta H (\text{Jg}^{-1})$ | 110.2 | 32.8 | 65.5 |

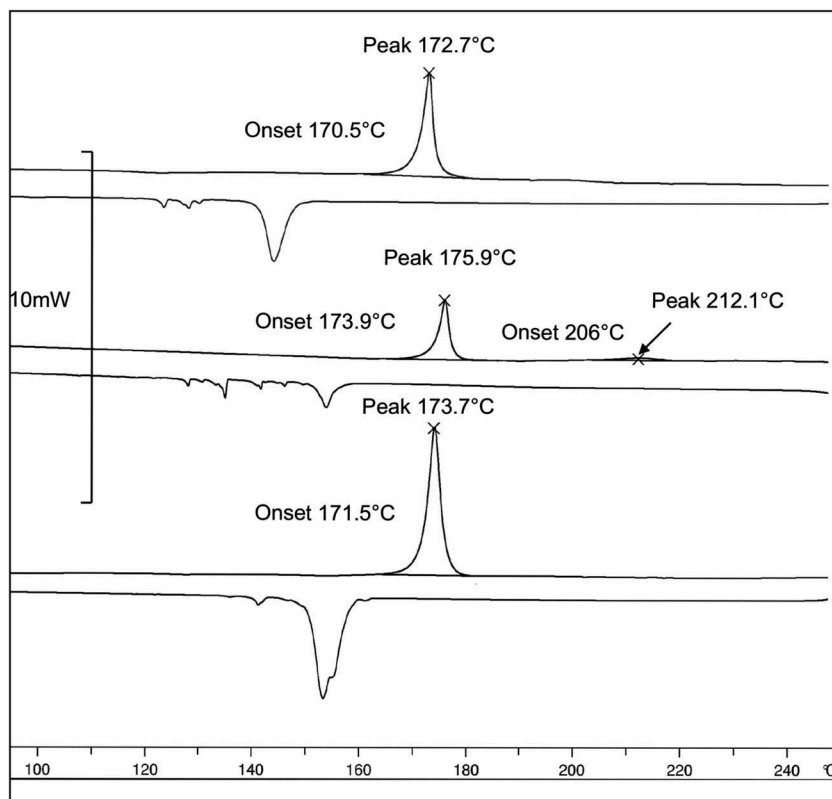


Figure 10. The DSC thermograms as a function of temperature (°C) for mixtures **Mix-12** (top), **Mix-13** (middle) and **Mix-14** (bottom).

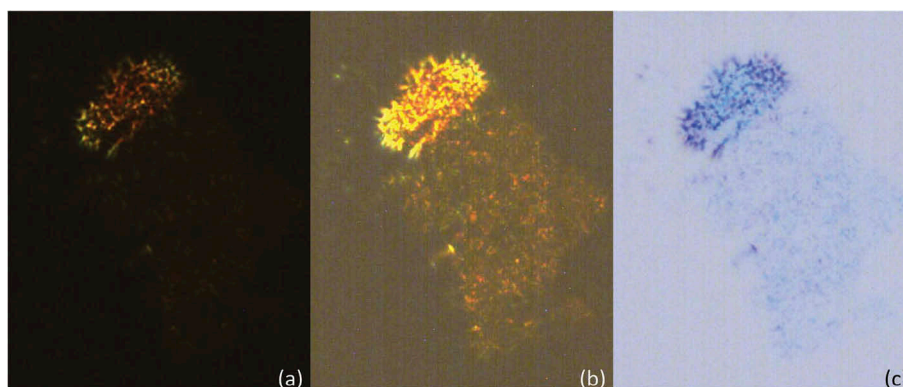


Figure 11. (Colour online) Photomicrographs of **Mix-13** (x100) showing (a) the original photomicrograph of dark texture of the mixture at approximately 200°C; (b) over exposed photomicrograph for the same texture at the same temperature and (c) colour inverted photomicrograph showing more detail of the texture.

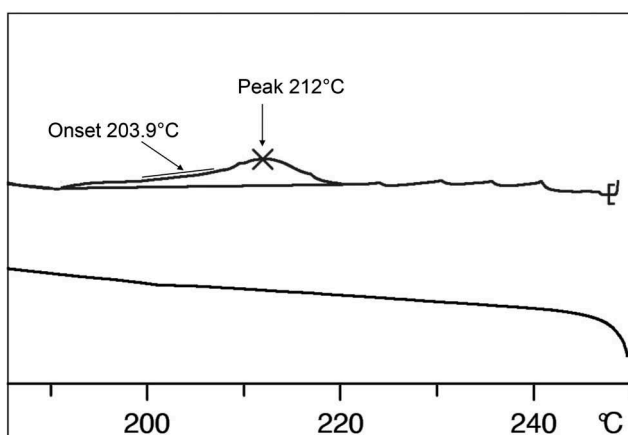


Figure 12. The DSC thermogram showing the transition for the unidentified intermediate phase of **Mix-13** to the isotropic liquid on heating. (The periodic peaks shown above the phase transition are artefacts of the sample bubbling up the sides of the sample pan.)

system is an interesting question? Truxene is slightly different to the other hard-disc materials in that it has some aliphatic characteristics associated with three CH_2 groups in the inner part of the core. These will have the ability to prevent to some degree the face-to-face interactions in a similar way to interannular twisting causes steric repulsion for *p*-sexiphenyl or by steric repulsion as found for the methyl substituted sexiphenyl shown in [Figure 4](#).

These results although indicating that a novel phase may have been found, its nature and structure, however, remain elusive, and the only theoretical model that fits with the experimental studies is that of a cubatic phase [37]. The cubatic phase structure and the simulations of hard discs fit with a slight disordering of the packing of the discs, which would be caused by the introduction of truxene into the mixture. Further studies however are required in order to elucidate this study.

Co-miscibility of nematogenic disc-like triphenylene derivatives

It is expected that materials exhibiting liquid-like nematic phases will show co-miscibility with similar systems [36]; however, there are very few examples of such studies being performed, and even fewer for co-miscibility experiments on columnar phases. For the studies given above, there is a need to confirm that miscibility experiments are valid for disc-like materials just as they are for rod-like systems. Therefore we undertook two studies, first to investigate the co-miscibility of nematic discotic phases, and second to make a similar study for columnar phases. Although not reported here, we have made a number of other experiments using structurally different discogens, the results from which support the results obtained in the following sections.

As the studies reported above were based on standard triphenylene materials, an experiment on the co-miscibility of nematogenic discotics was performed between nematogenic triphenylenes **3** and **4**, see [Figure 13](#) [38–40]. Although these chemically related materials exhibit nematic phases, neither appears to show columnar phases. The lateral aliphatic substituents in the peripheral phenyl rings cause out-of-plane twists of the peripheral rings relative to the triphenylene core unit, as shown in the Chemdraw model for compound **3** in [Figure 14\(a\)](#). The face-to-face steric repulsions favour the formation of nematic phases, and at the same time suppresses the formation of columnar structures. Thus, we performed more detailed geometry optimisations on isolated molecule of compound **3** using the mixed ONIOM method as implemented in Gaussian G09¹ with the DFT(B3LYP/6-31G(d) method for the aromatic core and the semi-empirical PM6 method for the aliphatic chains. Previously, we have shown that the PM6 method gives more than acceptable accuracy in reproducing methylene–methylene torsional barriers,

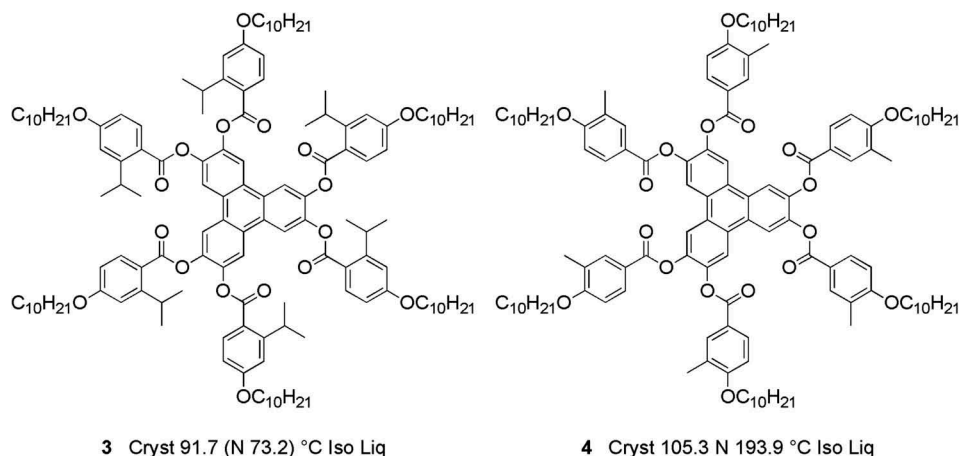


Figure 13. The chemical structures and phase transitions of compounds **3** and **4** [33,38].

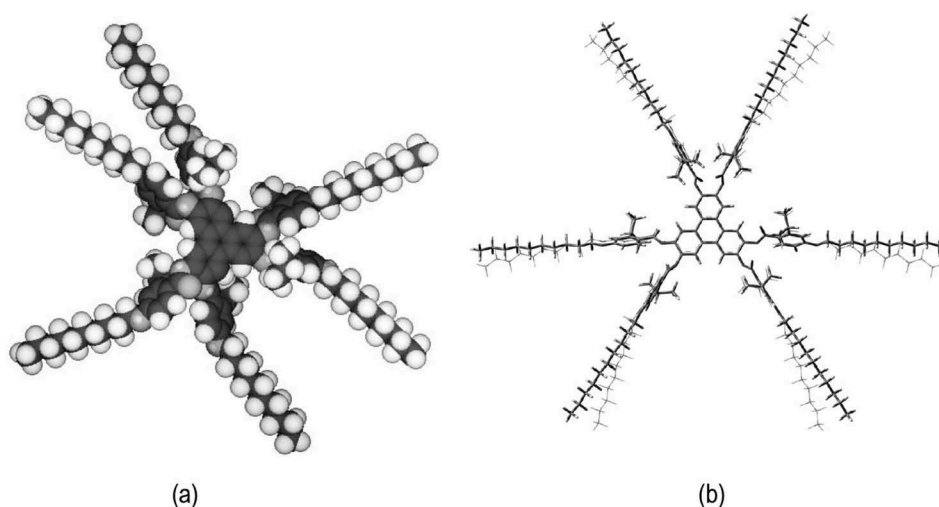


Figure 14. (a) Chemdraw model of Compound **3** showing the outer phenyl rings being twisted out of the plane with the central core unit. (b) Overlaid DFT(B3LYP/6-31G(d)) (solid) and ONIOM(B3LYP/6-31G(d):PM6) (wireframe) geometries for compound **3**; using the mixed ONIOM method decreases CPU time while giving a reasonably consistent result, the major difference being alkyl chain orientation. Both calculations were performed on an identical system (Intel (USA) Xeon E5-2680v4, 6 cores, 36 GB RAM) using Gaussian G09e01.

whereas being orders of magnitude faster than pure DFT calculations [41], dividing the molecule in this way into aromatic and aliphatic portions, allows us to accurately and quickly obtain optimised geometries as shown in Figure 14 (b). Thus, the simulations are in agreement, and show that the molecular architectures for compound **3** and *inter alia* Compound **4**, have sterically repulsive architectures that increase disc disordering, thereby favouring the formation of nematic phases.

We observed the disc diameters for compounds **3** and **4** were found to be similar with the diameter of compound **4** determined to be 46.0 Å, and the diameter of compound **3** 42.0 Å. Consequently, it was expected that the two materials would readily mix. Therefore, a binary phase diagram was constructed by determining the

transition temperatures and phase classifications of mixtures by a combination of optical microscopy and DSC. The phase diagram is shown in Figure 15 along with photomicrographs at various concentrations.

The phase diagram shows that the two nematogens are indeed co-miscible across the entire concentration range, with only a small dip in the N-I at around 40 mol% of compound **4** in the mixture. The included photomicrographs are all typical of the *schlieren* and planar textures of the nematic phase, with both two- and four-brush singularities present indicating that the phase is not biaxial, and thereby confirming the classification of the phase as nematic. The solidification curve however exhibits some abnormalities. For example, there was no major depression in the curve, below 60°C at 30 mol% of **4**, to

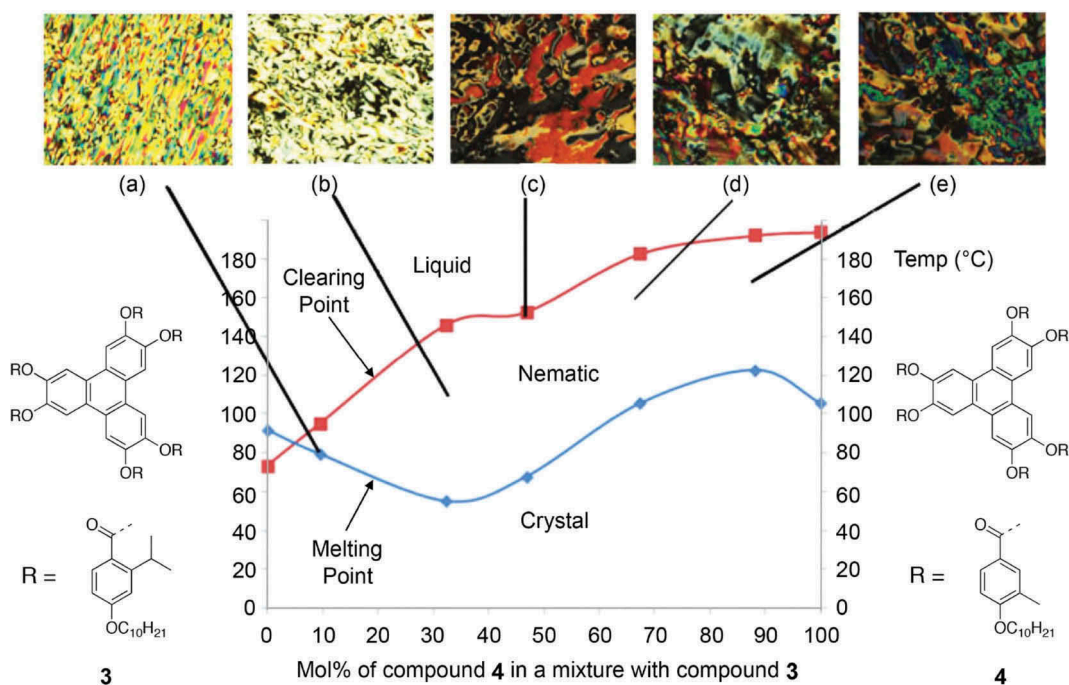


Figure 15. (Colour online) The Gibbs diagram for the binary mixtures of compounds **3** and **4**. Photomicrographs ($\times 100$) showing representative optical textures for the various mixture of compound **3**: (a) 9.5 mol% of compound **4** on cooling, 79.7°C – nematic; (b) 32.3% mol% of compound **4** on cooling, 112.6°C – nematic; (c) 46% mol% of compound **4** on cooling, 14°C – nematic; (d) 67.3% mol% of compound **4** on cooling, 146°C, – nematic; (e) 88.0% mol% of compound on cooling, 171.4°C – nematic.

give conventional eutectic behaviour, and moreover there was an increase in the solidification temperature at around 90 mol% of compound **4**; therefore, more detailed investigations were made of this behaviour by DSC, as shown in Table 5.

For the DSC results, the peak maxima were recorded rather than the tangents drawn at the maximum changes in the heat flow because of the broadness of the peaks for various mixtures. For the pure compounds, the clearing point enthalpy for **4** was found to be twice the size of the enthalpy for compound **3**. This is probably because compound **3** possesses lateral *ortho*-isopropyl groups as opposed to *meta*-methyl, which induce greater twisting of the peripheral phenyl rings thereby increasing the disordering in the system.

Using a related form of the Schröder-van Laar equation [42–44], the predicted composition of the eutectic mixture (**Mix-E**) was found to be 67.7 mol% of **3** and 32.3 mol% of **4**. This mixture was prepared and its phase behaviour was determined experimentally by POM and DSC, for which the results give a clearing point of 146–147°C. The melting point of the eutectic mixture determined from the Schröder-van Laar equation was found to be very close to minimum value of the melting curve of approximately 35 mol% of **4** in the phase diagram and a temperature of approximately 58°C.

In order to examine the reversibility of the phase transitions, and thereby to investigate the degree of the range of the biphasic properties in the phase diagram, a plot of the nematic to liquid peak transition

Table 5. Mixture compositions (mol%) and nematic to isotropic transition temperatures (°C) and enthalpies (Jg^{-1}) both on heating and cooling for binary mixtures of **3** and **4**. (The error for the temperature by DSC was $\pm 0.2^\circ\text{C}$, the error for enthalpies determined by DSC was $\pm 0.40 \text{ Jg}^{-1}$ and the error for the temperature determination by POM was $\pm 0.1^\circ\text{C}$).

| Compd/Mixture | Compd 4 (mol%) | N-Iso Liq | |
|-------------------------|----------------|--|--|
| | | Heating (°C) Enthalpy (Jg^{-1}) | Cooling (°C) Enthalpy (Jg^{-1}) |
| 3 | 0 | 74.4 ($\Delta H = 0.1$) | 74.1 ($\Delta H = -0.1$) |
| Mix-15 | 9.5 | 96.1 ($\Delta H = 0.1$) | 95.8 ($\Delta H = -0.1$) |
| Mix-E (Eutectic) | 32.3 | 147.3 ($\Delta H = 0.1$) | 146.6 ($\Delta H = -0.1$) |
| Mix-16 | 46.8 | 154.4 ($\Delta H = 0.2$) | 153.9 ($\Delta H = -0.2$) |
| Mix-17 | 67.3 | 183.4 ($\Delta H = 0.2$) | 183.0 ($\Delta H = -0.3$) |
| Mix-18 | 88.0 | 192.8 ($\Delta H = 0.3$) | 192.5 ($\Delta H = -0.6$) |
| 4 | 100 | 194.4 ($\Delta H = 0.2$) | 194.4 ($\Delta H = -0.2$) |

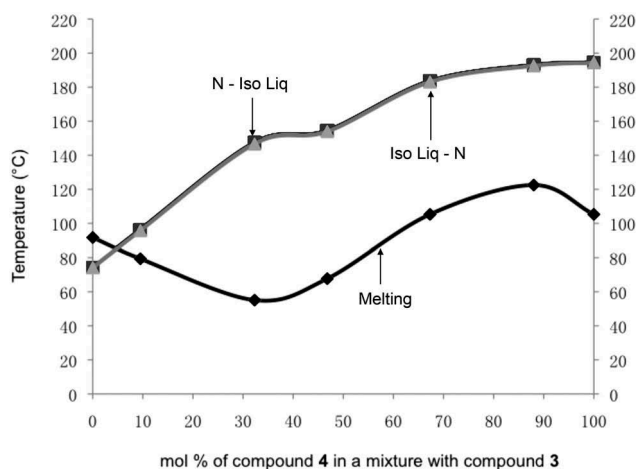


Figure 16. Phase diagram showing the biphasic region between heating and cooling cycles for the nematic to isotropic liquid transition for mixtures between compound **3** and compound **4**. The light-grey curve is for transitions from the liquid to the nematic phase on cooling, and the darker grey line just appearing above the light-grey curve is for the nematic to liquid transition on heating.

temperatures given in Table 5 was made, as shown in Figure 16. The temperatures for the heating and cooling cycles for the various mixtures virtually overlay one another, indicating a minimal extent for the biphasic region. This indicates that the two materials mix almost ideally as expected from the evaluation of their relative molecular architectures. Furthermore, the solid to liquid crystal phase transition curve accurately shows a depression associated with eutectic behaviour that is in agreement with the related Schröder-van Laar equation prediction. However, it should be noted that the eutectic depression is relatively lower than might be expected for liquid crystal systems.

In order to examine the relative stabilities of the nematic phases formed by binary mixtures and those of the pure components, a plot of the enthalpies of the clearing points as a function of temperature was created as shown in Figure 17. This figure does indeed show that the greater the percentage of compound **4** in the mixture, the more stable the nematic phase becomes, so much so that even a 90 mol% concentration of **4** with 10 mol% of **3** is more stable than pure compound **4**. In other words, the addition of compound **3** to compound **4** increases the disordering caused by the twisting of the peripheral rings induced by the isopropyl groups of compound **3** and thereby the nematic phase becomes stabilised.

As shown in Figure 15, there is also a significant increase of the melting point around the 10 mol% of compound **3** in the binary mixtures, which mirrors the isotropisation transition and is accompanied by an increase in enthalpy. Conversely, there is also an increase

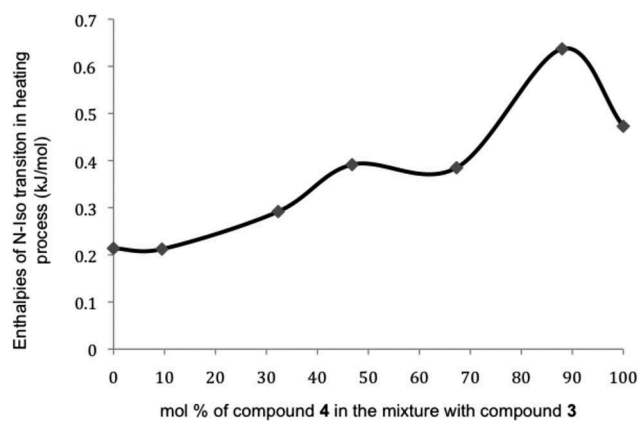


Figure 17. Enthalpies (kJmol^{-1}) for the nematic to isotropic liquid transitions on heating for mixtures of **3** and **4**.

in the enthalpy of the clearing point in the region of 53 mol % of compound **3** in the mixture, but this is accompanied by a depression in isotropisation temperature and little or no change to melting temperature. The first set of observations suggests that there could be an additional interaction occurring at the 10 mol% point, both in the solid state and in the mesophase, whereas for the second set there appears to be competition between the components that suppresses clearing point, but which supports the solid state. These results demonstrate that the interactions in the solid state are not necessarily so important to the liquid crystal phases, which confirms what is known about paramorphosis – that the solid state does not necessarily influence phase transitions and behaviour in the liquid crystal state, and that there must be donor–acceptor core–core interactions arising from different local charge distributions that is maximised for certain concentrations, as discussed later. These studies suggest that the phase diagrams for nematic discotic systems exhibit similar behavioural properties as those for rod-like systems, but that the melting behaviour is not necessarily typical of conventional solids.

Co-miscibility of disc-like columnar triphenylene derivatives

In this study, we examine the co-miscibility of substituted triphenylenes that exhibit columnar but not nematic phases. The structures and phase transitions of the materials for this study, **5** and **6**, are shown in Figure 18. In both cases, geometry optimisations performed with the mixed DFT(B3LYP/6-31G(d))/PM6 method (ONIOM, Gaussian G09e01) show that the peripheral rings are twisted out of the plane of the triphenylene core. This twist is thought to assist in the columns being disordered along the column axes, thereby supporting the formation of columnar disordered phases.

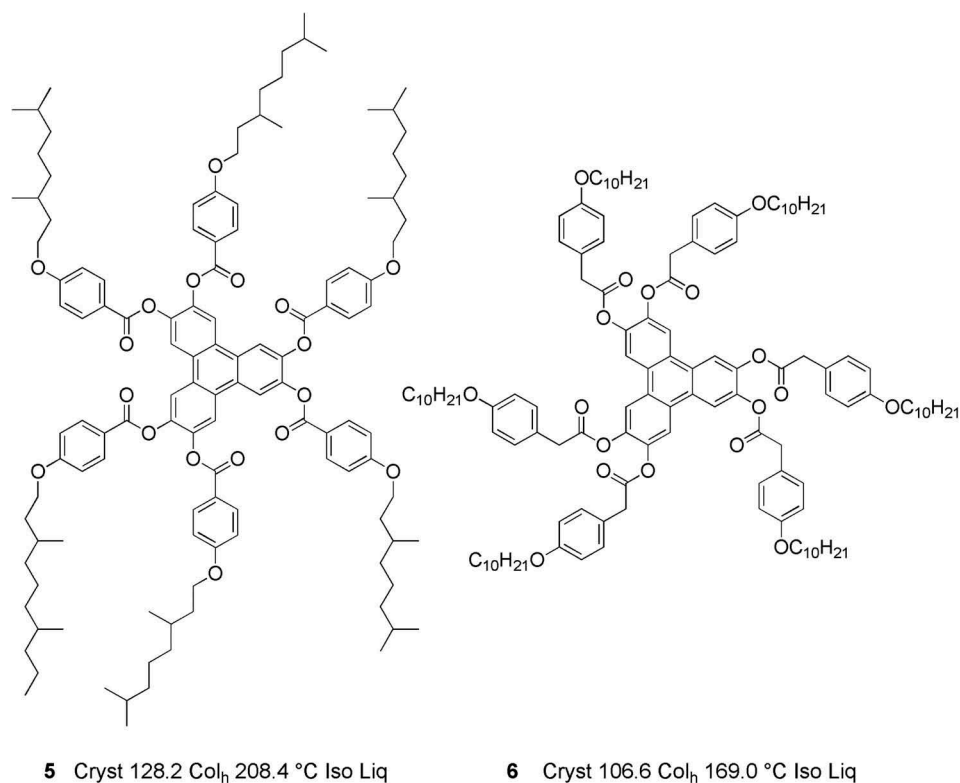


Figure 18. The chemical structures and phase transitions of columnar mesogens **5** and **6**.

Table 6. Mixture compositions (mol%) and phase transition temperatures (°C) and enthalpies (J/g) both in heating and cooling session for binary mixtures of **5** and **6**.

| Compd/Mixture | 5 (mol%) | Melting (°C) Enthalpy (Jg ⁻¹) | Col _h -Iso | |
|-------------------------|----------|---|---|---|
| | | | Heating (°C) Enthalpy (Jg ⁻¹) | Cooling (°C) Enthalpy (Jg ⁻¹) |
| 6 | 0 | 106.6 (ΔH = 10.8) | 176.7 (ΔH = 2.6) | 174.9 (ΔH = -2.3) |
| Mix-19 | 19.6 | 100.5 (ΔH = 9.8) | 142.5 (ΔH = 0.4) | 139.6 (ΔH = -0.4) |
| Mix-20 | 38.6 | 88.2 (ΔH = 5.2) | 122.7 (ΔH = 1.4) | 119.4 (ΔH = -1.5) |
| Mix-21 | 56.1 | 81.0 (ΔH = 1.6) | - | - |
| Mix-22 | 68.2 | 89.3 (ΔH = 2.9) | 169.6 (ΔH = 1.6) | 158.9 (ΔH = -1.4) |
| Mix-E (Eutectic) | 78.3 | 76.9 (ΔH = 1.0) | 183.5 (ΔH = 2.5) | 179.3 (ΔH = -2.4) |
| Mix-23 | 84.9 | 91.7 (ΔH = 0.3) | 180.3 (ΔH = 1.8) | 173.5 (ΔH = -2.0) |
| 5 | 100 | 133.5 (ΔH = 12.3) | 209.7 (ΔH = 5.4) | 205.7 (ΔH = -6.3) |

A series of mixtures of compounds **5** and **6** were prepared, and the phase behaviours were examined by POM and DSC; the transition temperatures determined by DSC are collected in [Table 6](#). As before, the composition of the predicted eutectic mixture (**Mix 23-E**) was determined via the Schröder-van Laar equation with a value of 78.3 mol% for compound **5** being found. The results for the phase behaviour of the experimental eutectic mixture, determined by DSC, are shown in [Table 6](#).

The binary phase diagram for mixing compound **5** with compound **6** is depicted in [Figure 19](#), along with photomicrographs of the detect textures at various concentrations and temperatures. The diagram shows that, even though both compounds exhibit hexagonal columnar phases, upon mixing the hexagonal columnar to the isotropic liquid phase,

transitions are suppressed rapidly and disappear in the centre of the phase diagram. The range for immiscibility was found to be 38–56 mol% of compound **5**. At the predicted eutectic concentration, there is only a weak depression in the melting point curve, and that the curve behaves anomalously in relation to conventional eutectic behaviour. This behaviour is exemplified in [Figure 19](#) where the texture, or lack of a texture, appears for the mixture at the centre of the phase diagram. Thus, the phase diagram reveals unexpected behaviour, and it also demonstrates that the isotropic to columnar transition does not behave in a comparable way in relation to phase diagrams of calamitic nematic or smectic phases. The behaviour appears more like the classical behaviour for the melting of soft crystals.

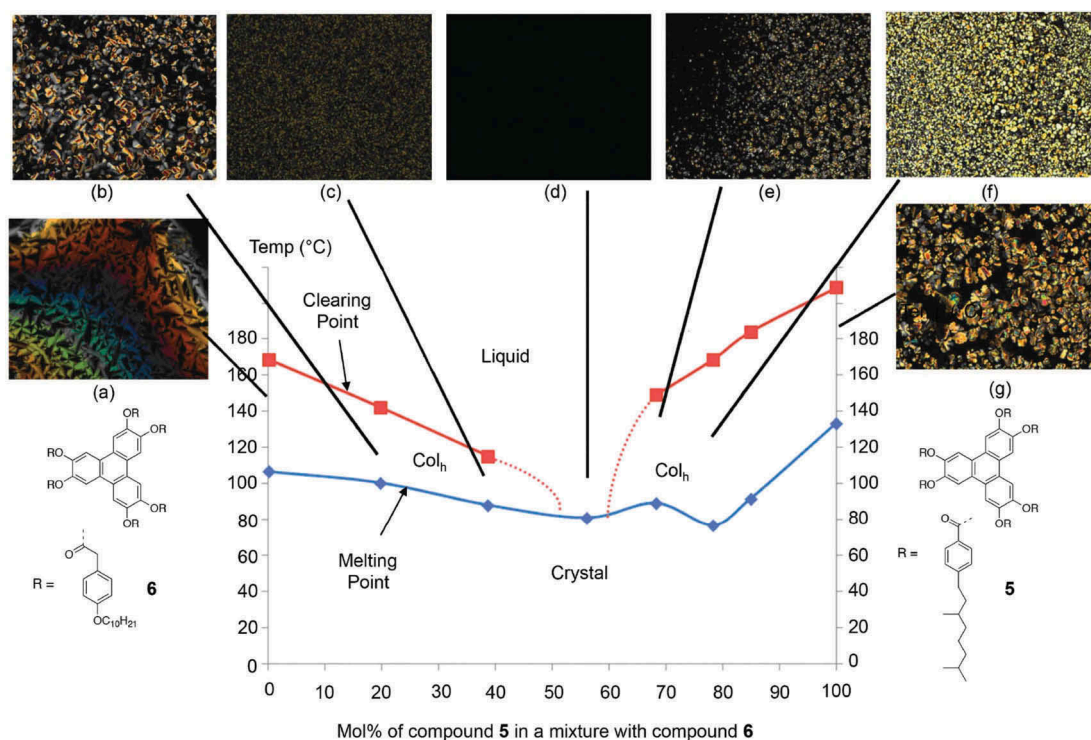


Figure 19. (Colour online) The phase diagram for the binary mixtures series of **5** and **6**. Photomicrographs ($\times 100$ magnification) showing representative optical textures for various mixture: (a) **6**, cooling, 147.5°C - Col_h ; (b) 19.6% cooling, 113.8°C , Col_h ; (c) 38.6% cooling, 110.2°C , Col_h ; (d) 56.1%, cooling, 110.0°C - non-mesogenic; (e) 68.2%, cooling, 135.0°C , Col_h ; (f) 78.3%, cooling, 165.1°C , Col_h ; (g) **5**, cooling, 186.3°C , Col_h .

Another possibility is that the observations of the depression in the clearing point transitions could be due to phase segregation between the two compounds. However, the transition temperatures to the solid state across the concentration range vary almost linearly with respect to the concentration. This observation suggests that the two materials ideally mix and do not segregate. Again this shows that the system is acting more like a classical phase diagram for two solids, where the Solid A–Solid B line is the equivalent to the melting point curve in the phase diagram.

In order to investigate this behaviour further, and to obtain accurate values for the transition temperatures on heating and cooling for the mixtures in the phase diagrams, calorimetric studies were performed for each individual mixture as shown in the Table. Biphasic behaviour in the phase diagram was examined by plotting the transition temperatures for heating and cooling together (Figure 20). Little biphasic behaviour was observed indicating that the two materials readily mix, and that the depression in the liquid to columnar phase transition is real. The enthalpic DSC studies tend to support these observations, and that no extra peaks were found for the liquid crystal underlying the

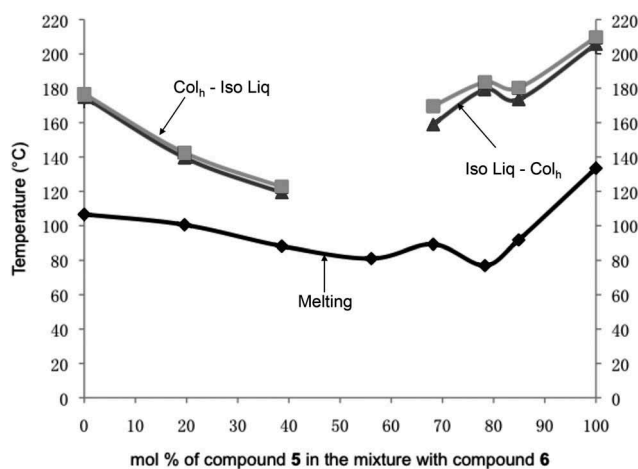


Figure 20. The phase diagram for mixtures of compounds **5** and **6** showing the biphasic region between heating and cooling cycles for the hexagonal columnar to isotropic liquid transition. In addition, the solidification curve is included.

columnar phase around the centre of the phase diagram as shown in Figure 21.

From these studies, it appears that the miscibility of columnar mesophases is unlikely, and that the phases behave more like soft crystals rather than liquid crystals.

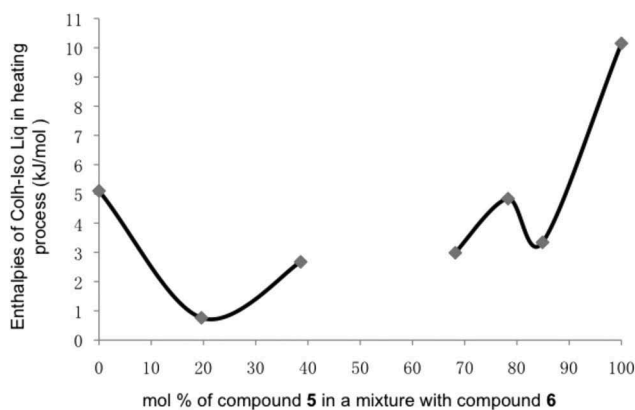


Figure 21. Diagram showing the enthalpies (kJmol^{-1}) for the columnar phase to isotropic liquid transitions on heating cycles for binary mixtures between compounds **5** and **6** as a function of the concentration of **6** (mol%).

This will have repercussions for applications of mixed discogens.

Discussion and conclusion

In the various studies performed in this report, phase diagrams and co-miscibility have been used in a traditional way in determining phase transitions, virtual transition temperatures and eutectic points. This approach has been relatively successful except for columnar systems. Co-miscibility in phase diagrams has not been used extensively for discotics, although there have been studies where co-miscibility and phase classification have been established, for example for the homologous series of benzene-hexa-*n*-alkanoates [45]. For the alkanates, co-miscibility was used to establish that the homologues exhibited the same columnar phase type. Later, studies using admixtures with benzene, however, established that the phases exhibited had molecules that were tilted in their columns, i.e. Col_{rd} , rather than being hexagonal columnar as previously reported [46,47]. The studies also indicated that the phases possessed 2D lattice structures. As the original co-miscibility investigations were made between homologues of benzene-hexa-*n*-alkanoates rather than with other materials, admixing might have been expected. However, miscibility between 2D systems may not be expected to be universal, and therefore may not be transferable outside of homologous series. Therefore, in terms of transferable information and applicable science across the boundaries between calamitic and discotic liquid crystals, there may be few similarities to utilise, although the area of nematics seems applicable. However, apart from these, there are greater differences which mean that the development of a better understanding of the mesomorphic behaviour of discotic systems is needed.

Starting first with hard-disc particles, the mesogenic properties of hard discs in comparison rods are scant. No mesophases were found for small hard-disc systems, whereas for rods with large-enough aspect ratios, both nematic and smectic phases were found. Virtual phase transitions determined by extrapolations were found for the nematic phase, but not for columnar phases, and in the mixing of molecules possessing differing disc diameters, no phases were observed, with one exception the addition of truxene to mixtures appeared to induce novel phase behaviour. The twisting structure of truxene may cause intermolecular packing to be weakened, as is the case with the interannular twisting in polyphenyls, such as *p*-sexiphenyl, thereby allowing the molecules to diffuse more easily.

For columnar phases, again for hard discs, no phases were found for pure compounds, transitions by extrapolation, or in the preparation of eutectic mixtures. For amphiphilic disc-like systems, composed of hard-core centres and flexible surrounding aliphatic chains, columnar phases of materials with similar chemical structures appear immiscible. Similarly, hard-disc materials when mixed with amphiphilic disc-like systems appear to mix to some extent, but the determination of virtual transition temperatures is not usually possible.

One of the problems faced in the determination of low-temperature phase transitions has been the lack of classical eutectic behaviour, with most of the phase diagrams exhibiting melting curves that show no defined minima, thereby appearing as a solidus lines. In fact, many of the studies we have made have shown small multiple minima as a function of concentration. This behaviour is probably linked to strong face-to-face associations of the disc-like molecules. The hard discs or hard cores can self-associate (A–A and B–B) or opposing associate (A–B) in nematic and columnar phases. For columnar structures in binary phase diagrams, where the interactions are of similar strengths, there can be A–A, B–B and A–B interactions along the columns thereby leading to random associations. Alternatively when the opposing interactions are stronger, there can be A–B pairings dominating the structure (see Figure 22). These random and organised structures can dominate at certain concentrations of the two components, which would account for the multiple minima in the melting curve, and the lack of classical eutectic behaviour.

In the above discussion, there is an assumption that the molecules have similar disc diameters, but for a number of the studies reported this is not the case, particularly for binary mixtures of hard disc and disc-like amphiphiles, cf Figures 8 and 9. In Figure 9, the columnar phase must be composed of columns that have irregular cross-sectional structures/diameters, and therefore the packing of the

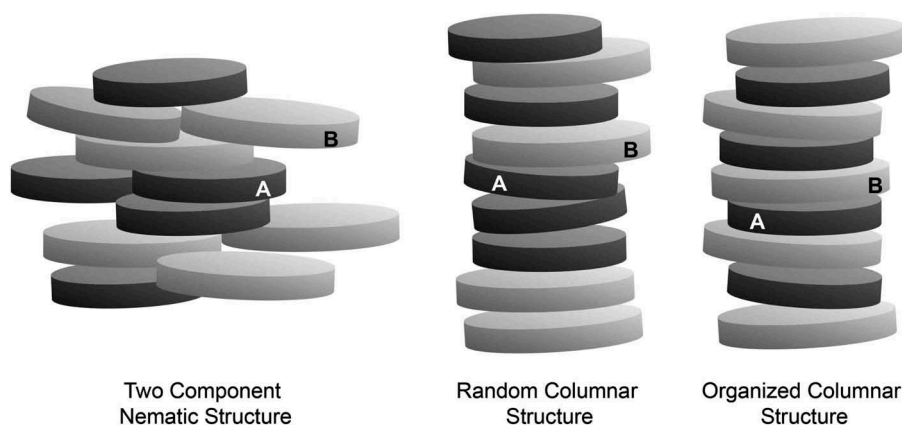


Figure 22. The various organisations of molecular discs in nematic and columnar phases. In the columnar phase, the strengths of face-to-face molecular interactions (A–A, B–B and A–B) can differ.

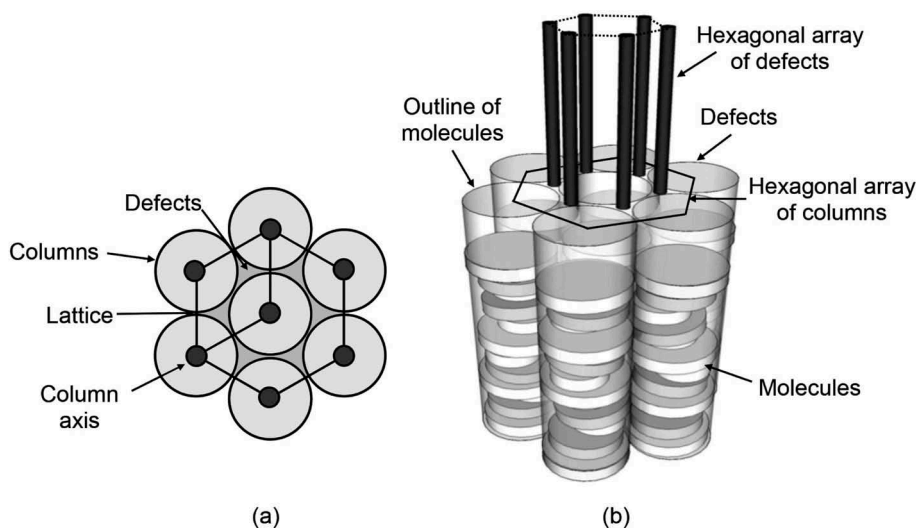


Figure 23. The lattice organisation for columnar mesophases composed of molecules of differing diameters.

columns into hexagonal arrays may be difficult. However, between the columns are defects which can also form into hexagonal arrays that are rotated by 30° to the molecular array, and hence also form 2D lattices, as shown in Figure 23. Thus, the columnar structure and phase will be stabilised by the defects in addition to the lateral packing of the molecular columns [24].

In summary, it is clear that discotic nematic phases exhibit typical properties associated with calamitic nematic phases, whereas the structural properties of calamitic smectics are not transferable to columnar phases.

Note

- Variations in the modelling and simulations of chemical structures were performed using either ChemDraw 3D or Gaussian 09, Revision E.01M. J. Frisch, G. W. Trucks, H. B. Schlegel, G. E. Scuseria, M. A. Robb, J. R. Cheeseman, G.

Scalmani, V. Barone, G. A. Petersson, H. Nakatsuji, X. Li, M. Caricato, A. Marenich, J. Bloino, B. G. Janesko, R. Gomperts, B. Mennucci, H. P. Hratchian, J. V. Ortiz, A. F. Izmaylov, J. L. Sonnenberg, D. Williams-Young, F. Ding, F. Lipparini, F. Egidi, J. Goings, B. Peng, A. Petrone, T. Henderson, D. Ranasinghe, V. G. Zakrzewski, J. Gao, N. Rega, G. Zheng, W. Liang, M. Hada, M. Ehara, K. Toyota, R. Fukuda, J. Hasegawa, M. Ishida, T. Nakajima, Y. Honda, O. Kitao, H. Nakai, T. Vreven, K. Throssell, J. A. Montgomery, Jr., J. E. Peralta, F. Ogliaro, M. Bearpark, J. J. Heyd, E. Brothers, K. N. Kudin, V. N. Staroverov, T. Keith, R. Kobayashi, J. Normand, K. Raghavachari, A. Rendell, J. C. Burant, S. S. Iyengar, J. Tomasi, M. Cossi, J. M. Millam, M. Klene, C. Adamo, R. Cammi, J. W. Ochterski, R. L. Martin, K. Morokuma, O. Farkas, J. B. Foresman, and D. J. Fox, Gaussian, Inc., Wallingford CT, 2016.

Acknowledgement

Many years ago when I was tasked to synthesise smectic C liquid crystals, there was little idea what molecular constraints

there were in material design. After struggling through many successful and unsuccessful preparations, I finally got out protractors and compasses and started modelling on a piece of graph paper. Fifteen years later, we had progressed to computer simulations. The gap between molecular and macro-molecular modelling was still immense, and our funders were posing me questions such as, “Can’t you model materials with suitable physical properties for applications without making them?” Today, we have a plethora of modelling possibilities to utilise, such as coarse grain modelling, Gay-Bern simulations and density functional theory. The gap has closed, and this has been due to Claudio’s underpinning research into the modelling of all brands of liquid crystals.

Thus, with our immense appreciation to Claudio for the many conversations we have had with him and the cross-disciplinary support that he has given to us as experimentalists; we dedicate our article to him. And from everyone here at York University, we wish him a very happy retirement.

Disclosure statement

No potential conflict of interest was reported by the authors.

Funding

This work was supported by the Engineering and Physical Sciences Research Council [grant number EP/L012375/1], [grant number EP/J007714/1] and [grant number EP/E064299/1]; the Leverhulme Trust, the European Science Foundation; Kingston Chemicals; DERA/QinetiQ; and the Wild Trust of the University of York.

ORCID

Richard Mandle  <http://orcid.org/0000-0001-9816-9661>
Stephen Cowling  <http://orcid.org/0000-0002-4771-9886>

References

- [1] Leadbetter AJ. Structural classification of liquid crystals. In: Gray GW, editor. Thermotropic liquid crystals. Critical reports on applied chemistry. Vol. 22; Chichester (UK): John Wiley & Sons; 1987. 1–27. ISBN 0-471-91504-1.
- [2] Gray GW, Goodby JW. Smectic liquid crystals – textures and structures. Glasgow and London: Leonard Hill; 1984. 153. ISBN 0-249-44168-3.
- [3] Cowling SJ, Davis EJ, Mandle RJ, et al. Defect textures of liquid crystals. Progress in liquid crystal science and technology. In: Kwok H-S, Shohei H, Ong L, editors. Singapore: World scientific, series in liquid crystals. Vol. 4, 2013. p. 55. ISBN: 978-981-4417-59-4.
- [4] Onsager L. The effects of shape on the interaction of colloidal particles. Ann NY Acad Sci. 1949;51:627–659.
- [5] Vroege GJ, Lekkerkerker HNW. Phase transitions in lyotropic colloidal and polymer liquid crystals. Rep Progr Phys. 1992;55:1241–1310.
- [6] Maier W, Saupe A. Eine einfache molekulare theorie des nematischen kristallinflüssigen zustandes. Z Naturforsch A. 1958;13:564–566.
- [7] Maier W, Saupe A. Saupe. Eine einfache molekular-statistische theorie der nematischen kristallinflüssigen phase 1. Z Naturforsch A. 1959;14:882–889.
- [8] Maier W, Saupe A. Eine einfache molekular-statistische theorie der nematischen kristallinflüssigen phase 2. Z Naturforsch A. 1960;15:287–292.
- [9] McMillan W. Simple molecular model for the smectic A phase of liquid crystals. Phys Rev A. 1971;4:1238–1246.
- [10] Leslie FM. Continuum theory for nematic liquid crystals. Cont Mech Thermodyn. 1992;4(3):167–175.
- [11] Cammidge AN, Bushby RJ. Synthesis and structural features. In: Demus D, Jw G, Gw G, et al., editors. Handbook of liquid crystals Vol 2B: low molecular weight liquid crystals II. Weinheim: Wiley-VCH; 1998. ISBN 3-527-29291-0, 693-748, and references therein.
- [12] Praefcke K, Kohne B, Singer D. Hexaalkynyltriphenylene: a new type of nematic-discotic hydrocarbon. Angew Chem Int Ed Engl. 1990;29:177–179.
- [13] Wöhrle T, Wurzbach I, Kirres J, et al. Discotic Liquid Crystals. Chem Rev. 2016;116:1139–1241.
- [14] Kawata K. Orientation control and fixation of discotic liquid crystal. Chem Rec. 2002;2:59–80.
- [15] Bushby RJ, Kawata K. Liquid crystals that affected the World: discotic liquid crystals. Liq Cryst. 2011;38:1415–1426.
- [16] Pisula W, Mullen K. Discotic liquid crystals as semiconductors. In: Jw G, Pj C, Kato T, et al., editors. Handbook of liquid crystals Vol 8: applications of liquid crystals. Weinheim: Wiley-VCH; 2014. Ch 20. 627–673. ISBN 978-3-527-32773-7.
- [17] Kaafarani BR. Discotic liquid crystals for opto-electronic applications. Chem Mater. 2011;23:378–396.
- [18] White J, Guthrie G, Gardner J. Mesophase microstructures in carbonized coal-tar pitch. Carbon. 1967;5:517–518.
- [19] Brooks J, Taylor G. The formation of graphitizing carbons from the liquid phase. Carbon. 1965;3:185–193.
- [20] Ichnatowicz M, Chiche P, Deduit J, et al. Formation de la texture des cokes de houilles et de brais etudiee par solubilite et par microscopie. Carbon. 1966;4:41–46.
- [21] Kipling J, Shooter P. Factors affecting the graphitization of carbon: evidence from polarized light microscopy. Carbon. 1966;4:1–4.
- [22] Honda H, Kimura H, Sanada Y. Changes of pleochromism and extinction contours in carbonaceous mesophase. Carbon. 1971;9:695–697.
- [23] Bisoyi HK, Kumar S. Carbon-based liquid crystals: art and science. Liq Cryst. 2011;38:1427–1449.
- [24] Vroeg GJ, Lekkerkerker HNW. Phase transitions in lyotropic colloidal and polymer liquid crystals. Rep Progr Phys. 1992;55:1241–1309.
- [25] Goodby JW, Mandle RJ, Davis EJ, et al. What makes a liquid crystal? The effect of free volume on soft matter. Liq Cryst. 2015;42:593–622.
- [26] Zafiroopoulos NA, Choi E-J, Dingemans T, et al. New all-aromatic liquid crystal architectures. Chem Mater. 2008;20:3821–3831.
- [27] Lewis IC, Kovac CA. Liquid crystal transitions of p-sexiphenyl. Mol Cryst Liq Cryst. 1979;51:173–178.

- [28] Wu X, Han J, Wang L. Palladium catalyzed C–I and vicinal C–H dual activation of diaryliodonium salts for diarylations: synthesis of triphenylenes. *J Org Chem.* **2018**;83:49–56.
- [29] Shimua T, Takenaka S, Murayama N, et al. Oxidation of pyrene, 1-hydroxypyrene, 1-nitropyrene and 1-acetylpyrene by human cytochrome P450 2A13. *Xenobiotica.* **2016**;46:211–224.
- [30] Liu P, Forni A, Chen H. Development of solvent-free ambient mass spectrometry for green chemistry applications. *Anal Chem.* **2014**;86:4024–4032.
- [31] Yuan MS, Fang Q, Liu ZQ, et al. Acceptor or donor (Diaryl B or N) substituted octupolar truxene: synthesis, structure, and charge-transfer-enhanced fluorescence. *J Org Chem.* **2006**;76:7858–7861.
- [32] Kestens V, Auclair G, Drozdowska K, et al. Thermodynamic property values of selected polycyclic aromatic hydrocarbons measured by differential scanning calorimetry. *J Therm Anal Calorim.* **2010**;99:245–261.
- [33] Zhong T. The thermodynamic behaviour and miscibility of discotic liquid crystals [PhD Thesis]. York. University of York; **2015**.
- [34] Béguin A, Billard J, Dubois J, et al. Discotic mesophases potentialities. *J Physique Colloq.* **1979**;40:C3-15-C13-16.
- [35] Destrade C, Tinh NH, Gasparoux H, et al. Disc-like mesogens – a classification. *Mol Cryst Liq Cryst.* **1981**;71:111–135.
- [36] Sackmann H, Demus D. The polymorphism of liquid crystals. *Mol Cryst Liq Cryst.* **1966**;2:81–102.
- [37] Duncan PD, Dennison M, Masters AJ, et al. Theory and computer simulation for the cubatic phase of cut spheres. *Phys Rev E.* **2009**;79:031702(1–11).
- [38] Hindmarsh P Investigation of the structure/property relationships in triphenylene discotic liquid crystals [PhD Thesis]. Hull. University of Hull; **1996**.
- [39] Hindmarsh P, Watson MJ, Hird M, et al. Effect of bulky lateral substituents on the discotic mesophase behaviour of triphenylene benzoates. *J Mater Chem.* **1995**;5:2111–2124.
- [40] Hindmarsh P, Hird M, Styring P, et al. Lateral substitution in the peripheral moieties of triphenylen-2,3,6,7,10,11-yl hexa-4-alkoxybenzoates: dimethyl-substituted systems. *J Mater Chem.* **1993**;3:1117–1128.
- [41] Archbold CT, Mandle RJ, Cowling SJ, et al. Conformational landscapes of bimesogenic compounds and their implications for the formation of modulated nematic phases. *Liq Cryst.* **2017**;44:2079–2088.
- [42] Iz S. Über die Abhängigkeit der Löslichkeit eines festen Körpers von seiner Schmelztemperatur. *Phys Chem.* **1893**;11:449–465.
- [43] van Laar JJ The possible forms of the melting point-curve for binary mixtures of isomorphous substances. *Proceedings of the Koninklijke Akademie Van Wetenschappen Te Amsterdam.* **1904**;6:244–262
- [44] Raynes EP. Mixed systems, phase diagrams, and eutectic mixtures. In: Jw G, Pj C, Kato T, et al., editors. *Handbook of liquid crystals Vol 1: applications of liquid crystals.* Weinheim: Wiley-VCH; **2014**. Ch 12. 351–363. ISBN 978-3-527-32773-7.
- [45] Billard J, Sadashiva BK. Miscibility studies of disc-like molecules. *Pramana.* **1979**;13:309–318.
- [46] Frank FC, Chandrasekhar S. Evidence of a tilted columnar structure for mesomorphic phases of benzene-hexa-n-alkanoates. *J Physique.* **1980**;41:1285–1288.
- [47] Singh S, Dunmur D. Liquid crystals of disc-like molecules. **2001**. Ch7, *Liquid crystals: fundamentals.* Singapore: World Scientific; 317. ISBN: 978-981-02-4250-3.